

Article

Not peer-reviewed version

A Comprehensive Study on Elasticity and Viscosity on Biomechanics and Optical Properties of the Living Human Cornea

[Francisco J. Ávila](#)^{*}, Oscar del Barco, [Maria Concepcion Marcellan](#), [Laura Remón](#)

Posted Date: 2 May 2024

doi: 10.20944/preprints202405.0095.v1

Keywords: Corneal biomechanics; Standard linear solid model; Corneal viscoelasticity; Corneal elasticity; Corneal viscosity; Corneal retardation time; Ccular hypertension; Ortho-K



Preprints.org is a free multidiscipline platform providing preprint service that is dedicated to making early versions of research outputs permanently available and citable. Preprints posted at Preprints.org appear in Web of Science, Crossref, Google Scholar, Scilit, Europe PMC.

Copyright: This is an open access article distributed under the Creative Commons Attribution License which permits unrestricted use, distribution, and reproduction in any medium, provided the original work is properly cited.

Article

A Comprehensive Study on Elasticity and Viscosity on Biomechanics and Optical Properties of the Living Human Cornea

Francisco J. Ávila ^{1*}, Óscar del Barco ², María Concepción Marcellán ¹ and Laura Remón ¹

¹ Departamento de Física Aplicada, Universidad de Zaragoza, 50009, Zaragoza, Spain.

² Laboratorio de Óptica, Instituto Universitario en Óptica y Nanofísica, Universidad de Murcia, Campus de Espinardo, 30100, Murcia, Spain.

* Correspondence: avila@unizar.es

Abstract: Corneal biomechanics is a hot topic in ophthalmology. The biomechanical properties of the cornea (BMPs) have important implications in the management and diagnosis of corneal diseases such as ectasia and keratoconus. In addition, the characterization of BMPs is crucial to model the predictability of a corneal surgery intervention, the outcomes of refractive surgery or follow-up of corneal diseases. The biomechanical behavior of the cornea is governed by viscoelastic properties that allow, among other structural implications, the damping of excess of intraocular pressure and reduce damage to the optic nerve. Currently, the most versatile and complete methods to measure corneal viscoelasticity are based on air-puff corneal applanation. However, those methods lack the ability to directly measure corneal viscosity. The aim of this work is to propose a new methodology based on the analysis of corneal air-puff measurements through the Standard Linear Solid model (SLSM) to provide analytical expressions to separately calculate the elastic and time-dependent (corneal retardation time and viscosity) properties. The results shown the mean values of elasticity (E), viscosity (η) and corneal retardation time (τ) in a sample of 200 young and healthy subjects. The influence of elasticity and viscosity on viscoelasticity, high-order corneal aberrations and optical transparency is investigated. Finally, the SLSM fed back from experimental E and η values was employed to compare the creep-relaxation response between normal, an ocular hypertension patient and Ortho-K user.

Keywords: corneal biomechanics; standard linear solid model; corneal viscoelasticity; corneal elasticity; corneal viscosity; corneal retardation time; ocular hypertension; ortho-K

1. Introduction

The hierarchical architecture of the cornea is responsible for structure and transparency due to its collagen-based lamellar organization [1,2]. X-ray scattering has revealed how the molecular collagen fibrils provide the mechanical properties of corneal tissue [3]. In particular, the spring-like and viscous crimp mechanisms are governed by the micro- and nanoscale collagen structure. The Elasticity of the cornea is enabled by the springs that straighten the supramolecular torsion of tropocollagen, while the viscosity responds to a curling mechanism of the fibrils [4]. In that sense, the cornea exhibits viscoelastic nature with differentiated elastic and time-dependent (viscous) properties.

Biomechanical properties (BMPs) of the cornea can be understood as the dynamic response of the cornea to applied external forces [5].

BMPs have revolutionized the anterior chamber subspecialty in ophthalmology, allowing powerful competition in the prognosis and diagnosis of surgery treatments [6] and corneal diseases [7], respectively. The main methodologies for in vivo assessment of corneal BMPs are based on air-puff tonometry [8], elastography [9] and Brillouin microscopy approaches [10]. The most widespread approaches include the Ocular Response Analyzer (ORA) [11] and corneal Scheimpflug visualization (Corvis-ST) [12] which consist of corneal applanation tonometry and provide the estimation of viscoelastic parameters and measurements of intraocular pressure (IOP).

Brillouin scattering allows the longitudinal modulus to be quantified from the analysis of Doppler Brillouin frequency shift [13]. This technique has successfully characterized biomechanical differences between normal, keratoconic and post-refractive surgery corneas [14] due to its abilities to observe the mechanical anisotropy of the cornea [10].

Elastography methods include magnetic resonance imaging, ultrasound elastography and the emerging optical coherence elastography [9] that provides micrometric scale measurements of corneal stiffness and structural properties. In this sense, our group recently reported a promising tool based on a sound pressure generator for in vivo observation of the biomechanical response of the cornea to low-frequency acoustic waves [15]. These methodologies mentioned above are in progress on how to perform a rapid non-invasive biomechanical assessment of the cornea with sufficient spatial resolution to also provide reliable structural information. Obtaining accurate measures of biomechanical parameters is essential for reliable predictability of mathematical models that reproduce the behavior of the cornea under normal and pathological conditions.

Under conditions of transient stress, the human cornea behaves as a viscoelastic material [16]. Various methods have been used mathematically model the viscoelastic nature of the human cornea, notably the Kelvin-Voigt, Maxwell and the Standard Solid models [17].

Glass et al. proposed a modified Kelvin-Voigt model to evaluate the effect of elastic and viscosity properties on hysteresis (measure of the viscoelastic damping of the cornea [18]) in a corneal phantom [19]. Su et al. proposed a hyper-viscoelastic approach combining the Mooney-Rivlin hyperelastic and modified Maxwell models for the specific simulation of trephine and suture in corneal surgery [20]. Whitford et al developed the first constitutive model for corneal viscoelastic representation by combining complex anisotropy, shear stiffness and fibrillar collagen density [21]. Recently, the Standard Solid model was proposed for the simulation of thermoviscoelasticity of the human cornea [22] due to its reasonable predictability for loads applied to the cornea on a constant or transient basics.

The study of corneal biomechanics through mathematical models achieves greater robustness if feedback with experimental data (or at least derivable from experimental measurements), is possible.

The aim of this work is to introduce a new methodology based on the analysis of air-puff corneal applanation measurements with the three-elements Standard Linear Solid Model (SLSM) to provide experimental analytical expressions to calculate separated elastic and time-dependent (i.e. viscous property and corneal retardation time) of the human cornea in vivo.

2. Materials and Methods

2.1. Participants

200 young, healthy volunteers participated in the study (mean age 21.07 ± 3.13 years old). None of them had a diagnosis of glaucoma, hypertensive ocular disease or undergone refractive surgery. In addition, a patient diagnosed with ocular hypertension (Intraocular pressure 24.8 mmHg) and an Ortho-K contact lens user were recruited to compare normal response from their variations in biomechanical properties in tensile creep-relaxation tests. The motivation to include a comparison with these two types of patients was the growing concern about glaucoma disease and to explore biomechanical complications of orthokeratology.

This study was reviewed by an ethical review board (Ethical Committee of Research of the Health Sciences Institute of Aragón, Spain. Reference C.P.-C.I.PI20/377.) according to the tenets of the Declaration of Helsinki. All participants were informed about the nature and risks of the study and signed an informed consent document.

2.2. In Vivo Corneal Assessment: Geometrical, Optical and Biomechanical Corneal Parameters

The Galilei Dual Scheimflug Analyzer (Galilei G2; Ziemer Ophthalmic Systems AG, Port, Switzerland) and the Ocular Response Analyzer device (ORA, Reichert Instruments, Depew, NY, USA) were used to measure geometrical and optical (optical density and corneal aberrometry)

corneal parameters, and biomechanical assessment of the living human cornea. Table 1 summarized the description of the parameters as a function of the employed technology.

Table 1. Geometrical (R_{cor} , CCT), optical (OD, SA, Trefoil and Coma), and biomechanical parameters (IOP_{cc} and CH) measured for morphometric, optical and biomechanical corneal assessment.

Parameter [Units]	Technology	Description
Rcor (mm)	Dual Scheimpflug analyzer	Mean corneal radii
CCT (μm)	Dual Scheimpflug analyzer	Central corneal thickness
OD (n.u)	Dual Scheimpflug analyzer	Optical density
SA(μm)	Dual Scheimpflug analyzer	Spherical aberration
Trefoil(μm)	Dual Scheimpflug analyzer	Trefoil term
Coma(μm)	Dual Scheimpflug analyzer	Coma term
IOP_{cc} (mmHg)	ORA	Corneal-compensated intraocular pressure
CH (mmHg)	ORA	Corneal hysteresis

The measurements were carried-out at the Visual Optics laboratory of the University of Zaragoza (Spain) by an experienced clinical optometrist. All data were incorporated into an Excel database without including more personal data than the date of birth and an identification code. Graphical representations and numerical simulations were carried-out using Origin Lab software (Origin Lab Corp., Northampton, MA, USA) and Matlab2019b (the MathWorks Inc., Natick, MA, USA) programming language.

2.3. The Three-Elements Standard Linear Solid Model

Figure 1 shows the three-elements Standard Linear Solid Model (SLSM) [23] which is obtained by adding a spring in series with a Kelvin-Voigt (KV) unit (blue box in Figure 1). The KV model consists of a spring coupled in parallel with a dash-pot that represents the viscoelastic component of the model. E is the elasticity of the springs, η is the viscosity of the dash-pot, σ the applied stress (or external load) and ϵ the strain, respectively. The third element consists of an extra spring (E_1) that forms the purely elastic behavior of the system.

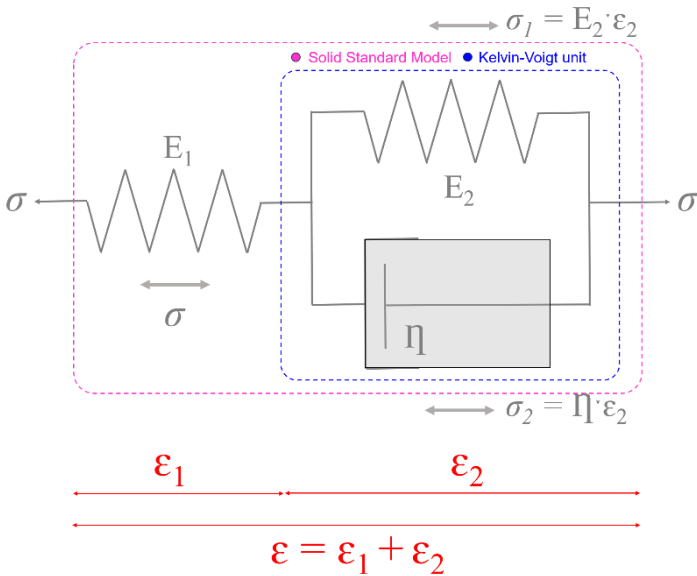


Figure 1. Representation of three elements of the standard linear solid model. E , η , σ and ϵ corresponds to elasticity, viscosity, applied stress and induced strain, respectively.

From the Figure 1, the equations for the SLSM are [23]:

$$\begin{aligned}\sigma &= \sigma_1 + \sigma_2 \\ \sigma &= E_1 \varepsilon_1 \\ \sigma_1 &= E_2 \varepsilon_2 \\ \sigma_2 &= \eta \dot{\varepsilon}_2 \\ \varepsilon &= \varepsilon_1 + \varepsilon_2\end{aligned}\quad (1)$$

Where $\dot{\varepsilon}$ is the stress rate. The constitutive law for the SLSM is given by [23]:

$$\sigma + \left(\frac{\eta}{E_1 + E_2} \right) \dot{\sigma} = \left(\frac{E_1 \cdot E_2}{E_1 + E_2} \right) \varepsilon + \left(\frac{E_1 \eta}{E_1 + E_2} \right) \dot{\varepsilon} \quad (2)$$

Assuming the cornea to be axisymmetric, a single elastic constant should govern the corneal behavior, so we can identify $E_1 = E_2$ [19]. Consequently, the constitutive law for the standard solid model can be written as:

$$\sigma + \left(\frac{\eta}{2E} \right) \dot{\sigma} = \left(\frac{E}{2} \right) \varepsilon + \left(\frac{\eta}{2} \right) \dot{\varepsilon} \quad (3)$$

If the SLSM is loaded (considering a step function for the stress σ), the response is given by solving the differential equation (Eq.3) for strain with initial condition $\varepsilon(0)=0$:

$$\varepsilon(t) = \sigma_0 \left[\frac{1}{E} + \frac{1}{E} \left(1 - e^{-\left(\frac{E}{\eta} \right) t} \right) \right] \quad (4)$$

When the stress is removed, the absence of load ($\sigma=0$) reduces the constitutive law to:

$$\left(\frac{E}{2} \right) \varepsilon + \left(\frac{\eta}{2} \right) \dot{\varepsilon} = 0 \quad (5)$$

and the relaxation response is:

$$\varepsilon(t) = \frac{\sigma_0}{E} e^{-\left(\frac{E}{\eta} \right) t} \left(e^{\left(\frac{E}{\eta} \right) t_u} - 1 \right) \quad (6)$$

Here, the time t begins with from the zero load event at which the stress is applied. The point at which the stress is removed is given by t_u . Then, equations 4 and 6 can predict the response of the model (strain) under stress given the values for elasticity and viscosity. The next section attempts to develop analytical expressions for the calculation of E and η from air-puff corneal applanation measurements.

2.3. Experimental Calculation of Elastic and Time-Dependent Biomechanical Properties

The ORA device provides invaluable mechanical information beyond the CRF, CH and IOP parameters provided by commercial software. Figure 2a shows a representative measurement showing both signals corresponding to the force of the air jet applied to the cornea and the deformation monitored by electro-optical detection. The red waveform shows two peaks (P1 and P2) representing the first and second applanation events as the cornea moves inward and outward, respectively. The green Gaussian-shaped curve corresponds to the delivered pressure and is responsible for the forward and backward corneal displacement phases. At the moment of maximum corneal deformation, the Gaussian reaches its maximum peak.

In that sense, Figure 2b represents the first applanation event where the applied stress (σ_{P1}) on the anterior corneal surface is given by [19]:

$$\sigma_{P1} = \frac{P_{r,1} \cdot R_{cor}}{2 \cdot CCT} \quad (7)$$

where R_{cor} and CCT are the original corneal radius and central corneal thickness, respectively. $P_{r,1}$ is the resulting pressure in the first applanation event [24]:

$$P_{r,1} = P_1 + P_{tf} - IOP \quad (8)$$

Here P_1 , P_{tf} and IOP are the first applanation pressure, the tear film surface pressure and the intraocular pressure, respectively. Once the measurement is completed, the cornea returns to its original state and shape (Figure 2c).

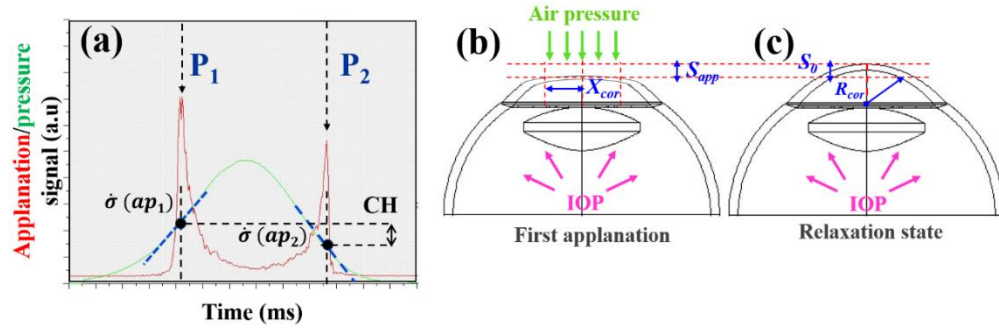


Figure 2. (a): Representation of the ocular anterior chamber during air-puff tonometry. S_0 and R_{cor} correspond to the sagitta of the area of air jet application and corneal curvature radius before appplanation. (b): At the first appplanation event, $S_{app}=S_0$. The diameter of the area of appplanation is given by $2 \cdot X_{cor}$. (c): representation of the appplanation/pressure signals during air-puff tonometry ORA measurement. P_1 , P_2 , CH , $\dot{\sigma}(ap_1)$ and $\dot{\sigma}(ap_2)$ are the first and second appplanation pressures, corneal hysteresis and first and second pressure rates at the moment of the two appplanation events, respectively.

The air jet applies stress on a total corneal diameter of $2 \cdot X_{cor}$ which subtends an arc length in the relaxed state, L_{cor} [19]:

$$L_{cor} = 2 \cdot CCT \left[\sin^{-1} \left(\frac{X_{cor}}{R_{cor}} \right) \right] \quad (9)$$

When the cornea is completely appplanated (i.e. corneal sagitta is S_{app}), $L_{cor} = L_{flatt} = 2 \cdot X_{cor}$, then the induced strain (ε_{flatt}) by the appplanation pressure P_1 can be calculated from eq. 4 [19]:

$$\varepsilon_{flatt} = \frac{L_{cor} - L_{flatt}}{L_{cor}} = \frac{X_{cor}}{CCT \cdot \sin^{-1} \left(\frac{X_{cor}}{CCT} \right)} - 1 \quad (10)$$

Once the values for stress σ_{P1} and strain ε_{flatt} for the first appplanation are known, corneal elasticity can be calculated:

$$E = \frac{\sigma_{P1}}{\varepsilon_{flatt}} \quad (11)$$

On the other hand, the corneal retardation time τ is the time in which about 63% of the final corneal strain is determined [25,26]. This metric would measure the cornea's ability to absorb IOP fluctuations. Recently, our group developed a theoretical method to derive a practical expression for this parameter [27], once the appplanation pressures (P_1 and P_2) and their first derivatives are known (please, see again Figure 2a):

$$\tau = \frac{2CH}{|\dot{\sigma}(ap_1)| + |\dot{\sigma}(ap_2)|} \quad (12)$$

Once the time-dependent parameter τ is computed, the corneal viscosity can be easily obtained by the following expression:

$$\eta = E \cdot \tau = 2 \cdot \frac{\sigma_{P1} \cdot CH}{\varepsilon_{flatt} \cdot (|\dot{\sigma}(ap_1)| + |\dot{\sigma}(ap_2)|)} \quad (13)$$

3. Results

3.1. Effect of IOP on Elastic, Viscoelastic and Viscous Properties of the Cornea

The aim of this section, is to investigate how fluid pressure within the eyeball impacts corneal biomechanics due to its relevance to glaucoma disease [28]. Table 1 shows the representative mean values of IOP, geometric and biomechanical parameters for all participants in this study. Elasticity, Tau and Viscosity were calculated using equations 11, 12 and 13, respectively.

Figure 3 represents CH as a function of the IOP. As the intraocular pressure increases, the ability of the cornea to absorb and dissipate excess of mechanical energy reflects a decrease in CH measurements with a significant negative correlation ($R^2=-0.49$, $p<0.001$).

Table 1. Mean values (\pm standard deviation) for the corneal-compensated intraocular pressure (IOP_{cc}), central corneal thickness (CCT), corneal radius (R_{cor}), corneal hysteresis (CH), elasticity (E), viscosity (η) and tau (τ) parameters.

IOP_{cc} (mmHg)	CCT (μm)	R_{cor} (mm)	CH (mmHg)	E (KPa)	η (Pa *s)	T (ms)
16.51 \pm 2.32	555.75 \pm 29.49	7.89 \pm 0.30	9.78 \pm 1.16	3.44 \pm 2.67	3.57 \pm 2.39	1.12 \pm 0.13

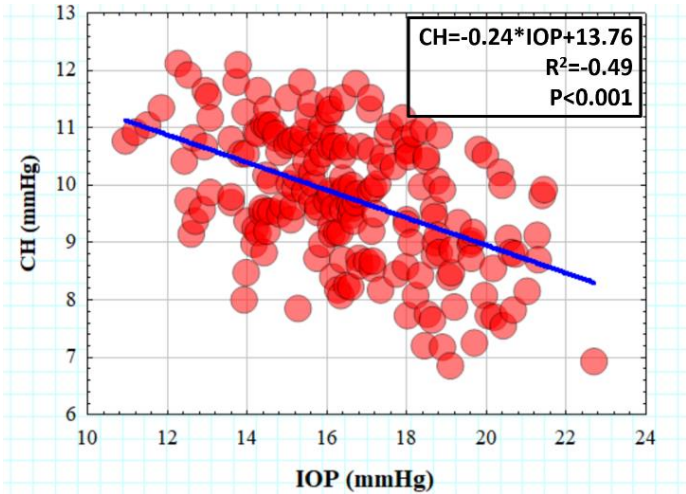


Figure 3. CH as a function of the IOP_{cc} for all participants involved in the study. The blue line corresponds to the best linear fitting of the negative correlation found between both variables.

Figure 4 shows the experimental values for Elasticity (Figure 4a) and Viscosity (Figure 4b) of the human cornea as a function of the IOP_{cc} . The results showed piecewise linear behavior with statistical correlations of $R^2=0.81$ ($p<0.0001$) and $R^2=0.80$ ($p<0.0001$), respectively.

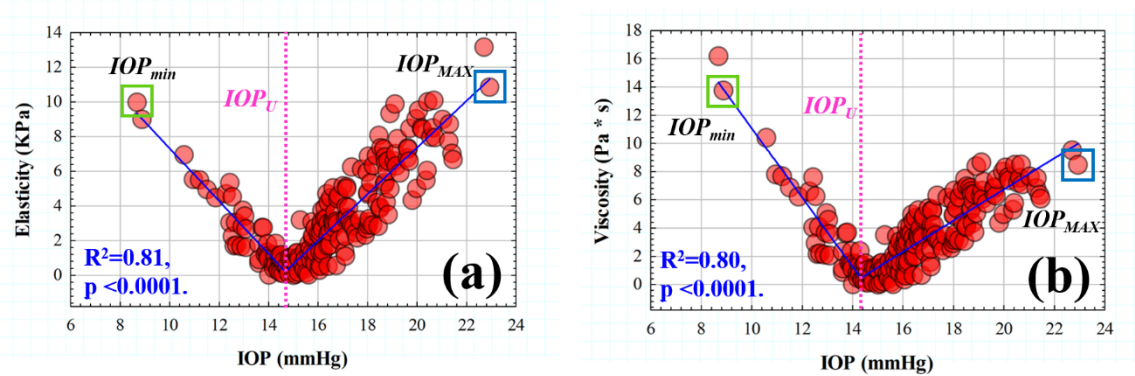


Figure 4. Elasticity (a) and viscosity (b) as a function of the intraocular pressure. The blue lines correspond to the piecewise linear fitted intervals. The green and blue boxes indicate the minimum (IOP_{min}) and maximum (IOP_{max}) IOP of the intervals separated by the IOP threshold (IOP_u).

The two-segment linear regressions for E and η are given by experimental fittings expressions 13 and 14. We found a threshold IOP value (IOP_u) of 14.45 mmHg for which the intervals are defined. For IOP values less than 14.45 mmHg, the elastic and viscous components of the cornea are negatively correlated: elasticity and viscosity decrease as the IOP increases up to IOP_u . However, for IOP values

higher than IOP_u the trend is reversed and both elastic and viscous properties increase as a function of IOP.

$$E(IOP) = \begin{cases} \frac{9.33 \cdot (IOP_u - IOP) + 0.21 \cdot (IOP - IOP_{min})}{IOP_u - IOP_{min}}, & IOP_{min} \leq IOP \leq IOP_u \\ \frac{0.21 \cdot (IOP_{MAX} - IOP) + 11.30 \cdot (IOP - IOP_u)}{IOP_{MAX} - IOP_u}, & IOP_u \leq IOP \leq IOP_{MAX} \end{cases} \quad (14)$$

$$\eta(IOP) = \begin{cases} \frac{14.33 \cdot (IOP_u - IOP) + 0.47 \cdot (IOP - IOP_{min})}{IOP_u - IOP_{min}}, & IOP_{min} \leq IOP \leq IOP_u \\ \frac{0.47 \cdot (IOP_{MAX} - IOP) + 9.98 \cdot (IOP - IOP_u)}{IOP_{MAX} - IOP_u}, & IOP_u \leq IOP \leq IOP_{MAX} \end{cases} \quad (15)$$

3.2. Retardation Time as a Biomechanical Behavior Threshold: Role of Elasticity and Viscosity on Corneal Viscoelasticity

Corneal retardation time (τ) has been reported as a good biomarker of corneal viscoelasticity [26] which, in collusion with the CH parameter, provides combined information of elastic and viscous properties. At this point, it is crucial to ask a fundamental question: What is the elastic response of the cornea when its viscoelastic behavior changes?

Figure 5 shows the elasticity calculated from all subjects as a function of the retardation time (τ). The elastic property of the cornea shows an almost symmetric behavior around a given value of the retardation time $\tau_u = 1.22$ ms. For those corneas characterized by a retardation time less than 1.22 ms, elasticity decreases as viscoelasticity increases. However, an inverse behavior is observed for values of $\tau \geq 1.22$ ms.

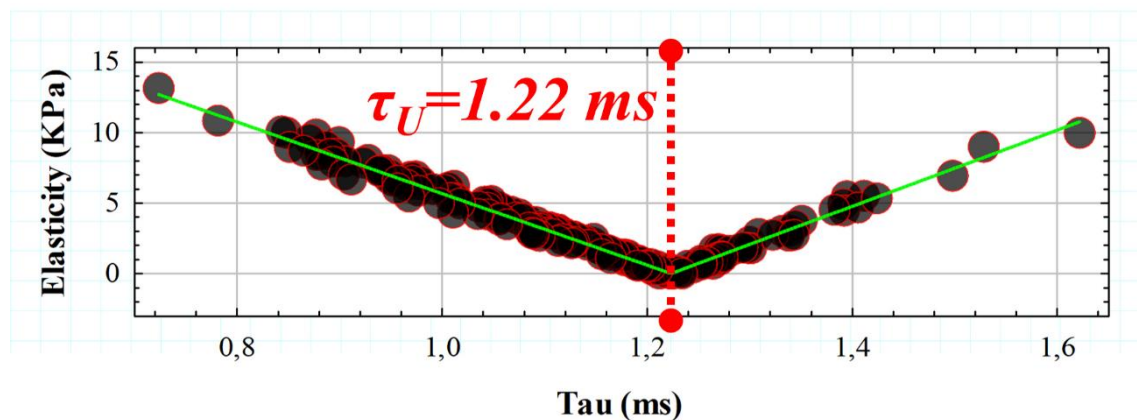


Figure 5. Elasticity as a function of the retardation time. The red dotted line indicates the threshold retardation time (τ_u) separating the trend intervals.

From the data observed in Figure 5, there appears to be a threshold in the retardation (τ) time beyond which the elastic behavior of the cornea is reversed. To understand the influence of this threshold on the evaluation of viscoelasticity, Figure 6 shows the influence of the elasticity and viscosity on corneal hysteresis for values of $\tau \leq 1.22$ ms (Figure 6a,b, respectively) and for values of retardation time greater than τ_u (Figure 6c,d). For retardation times less than 1.22 ms, both the elasticity (Figure 6a) and viscosity (Figure 6b) components contribute to an increase in corneal hysteresis with parabolic correlation ($R^2 = 0.60$ and $R^2 = 0.59$, respectively). However, an interesting phenomenon is observed for corneas exhibiting retardation times larger than 1.22 ms: If corneal viscosity (Figure 6c) or elasticity (Figure 6d) increases, the viscoelasticity measured by the CH parameter decreases with a statistically significant negative linear trend ($R^2 = -0.66$ and $R^2 = -0.14$, respectively). It is worth highlighting that while for $\tau \leq 1.22$ ms the corneal hysteresis shows a similar dependence on viscosity and elasticity, for retardation times greater than τ_u the main contribution to viscoelasticity comes from the viscous component.

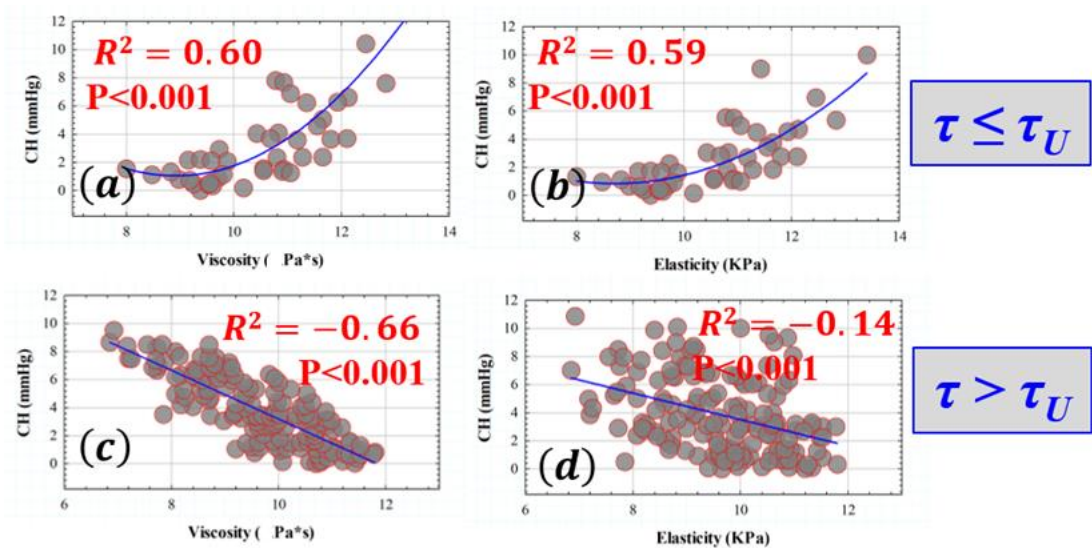


Figure 6. CH as a function of viscosity (a) and elasticity (b) for retardation time values below the threshold (τ_u) and CH versus η (c) and E(d) for suprathreshold τ values.

3.3. Influence of Elasticity and Time-Dependent Parameters on Corneal Optical Properties

The ultrastructure of the stromal lamellae (formed by type-I collagen fibrils) is responsible for corneal optical transparency [3], in addition the three-dimensional architecture at the microscopic level has an important implication for the corneal biomechanics [5]. In this sense, this section studies the influence of elasticity and time-dependent corneal properties on both corneal transparency (quantified by optical density measures) and high-order corneal aberrations.

Table 2 shows the representative mean values of optical density (OD), spherical aberration (SA), trefoil and coma terms of the study sample.

Table 2. Mean values (\pm standard deviation) for the OD, SA, trefoil and coma of all participating subjects.

OD (pd/ μ m)	SA (μ m)	Trefoil (μ m)	Coma (μ m)
0.034 \pm 0.004	-0.15 \pm 0.08	0.19 \pm 0.13	0.27 \pm 0.14

Figure 7 shows the relationships found between viscosity and corneal optical density (OD). Optical density increases moderately with viscosity ($R^2=0.28$) (i.e. optical transparency decreases as viscosity increases). No relationships were found between elasticity and optical density.

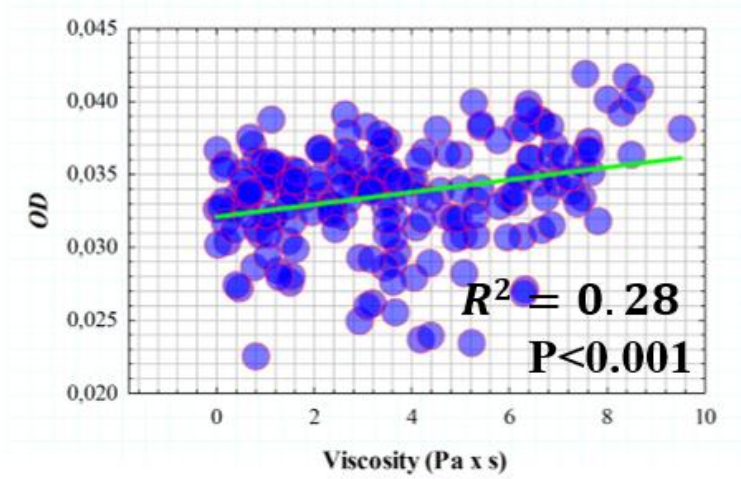


Figure 7. Optical density values as a function of the viscous component. Green line corresponds to the statistical linear fitting ($R^2=0.28$, $p<0.001$).

With respect to corneal optical imperfections measured by high-order aberrometry, Figure 8 shows the correlations found between elasticity and retardation time with the coma term. The data shown in Figure 8a indicate how an increasing in corneal elasticity correlates ($R^2=-0.23$) with a descent in the amount of coma term. On the contrary, longer retardation times are related to an increase in corneal coma (Figure 8b).

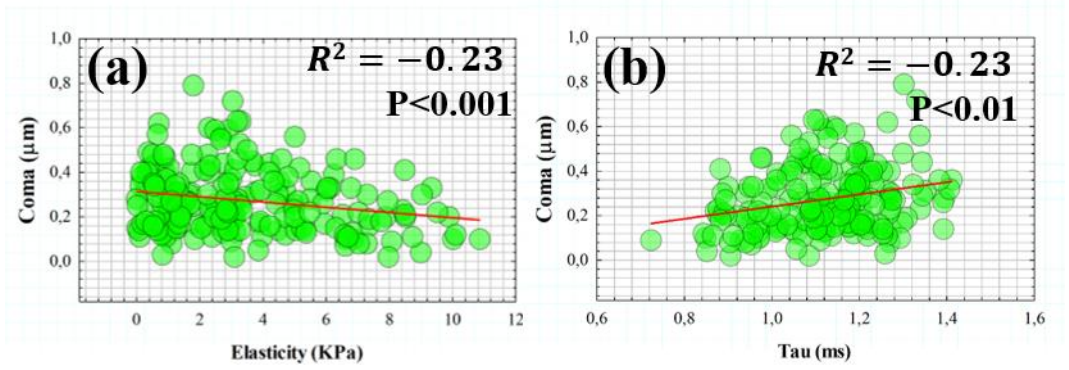


Figure 8. Coma high-order term as a function of elasticity (a) and corneal retardation time (b). Red lines corresponds to the best linear fittings of the data.

3.4. Creep-Relaxation Response of the Human Cornea as a Function of Elasticity and Viscosity

Once the elastic and time-dependent biomechanical properties of the human cornea are experimentally derived from ORA measures and Scheimpflug imaging, the SLSM (see Section 2.3) can be fed back from experimental data for the simulation of creep and stress-relaxation behavior under real conditions. Table 3 shows the experimental values of elasticity and viscosity for the representative mean value of our study sample, for an ocular hypertensive patient and a healthy user of Ortho-K contact lenses.

Table 3. Elasticity (E) and viscosity (η) for a normal cornea (mean value of 200 healthy subjects), for a ocular hypertensive patient and a healthy Ortho-K contact lens wearer.

	Normal cornea	Ocular hypertensive	Ortho-K user
E (Kpa)	3.44	13.23	3.13
η (Pa * s)	3.57	8.62	3.47

The data shown in Table 3 were entered as inputs into the Solid model to perform a creep and stress-relaxation response over a time of 10 seconds. The ocular hypertensive patient showed a drastic increase in both elastic (+42.2 %) and viscous (+82.85 %) components. However, the Ortho-K user experienced a slight reduction in E (- 9.44 %) and almost negligible variation in η (-2.84 %).

Figure 9 compares the creep-relaxation test between a pathological eye and ortho-k contact lens wearer with the normal response of a population of 200 healthy young subjects. In agreement with the mean values shown in Table 3, the Ortho-K wearer showed an almost negligible relaxation response compared to normal corneas, while a slightly weaker reduction is seen in creep response. The ocular hypertensive patient showed a rapid stabilization of the creep (Figure 9a) and relaxation curves (Figure 9b) with significantly reduced response compared to the normal representative curves (Figure 9, blue lines).

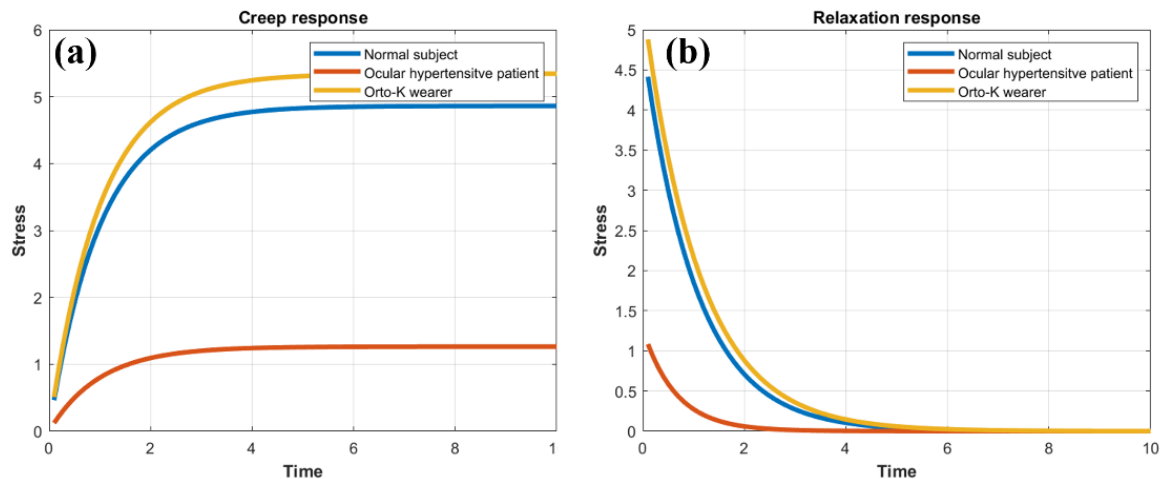


Figure 9. Comparative creep-relaxation tensile tests for normal corneas (blue curve), an ocular hypertensive patient (red curve) and an Ortho-K contact lens user (orange curve).

4. Discussion and Conclusions

We proposed a simple experimental methodology to obtain information on separated elastic and viscous components from the viscoelastic properties of the living human cornea. The results of Ocular Response Analyzer combined with geometric information from corneal Scheimpflug imaging allowed us to calculate the corneal retardation time [24] (τ), the corneal elasticity (E) and finally the corneal viscosity (η) from a large sample of young subjects.

In 2008, Glass et al [19] reported a methodology based on a viscoelastic model to evaluate how the individual contribution of viscous and elastic components affects corneal hysteresis (i.e. corneal viscoelasticity) in a corneal phantom.

To the best of our knowledge, this is the first work presenting the experimental derivation of viscous and elastic components from measurements of living human corneas combining non-contact tonometry and Scheimpflug imaging. In addition, we present analytical expressions to calculate both elastic moduli and time-dependent biomechanical properties of the human cornea.

The SLSM employed here to model the human cornea and obtain the creep and stress-relaxation response from experimental data by solving the constitutive stress-strain equation of the constitutive law for the loading and unloading conditions of the system.

Biomechanical and geometric experimental data from ORA measurements and Scheimpflug imaging were acquired from 200 eyes of healthy young subjects (See Table 1). From them, E (Kpa), τ (ms) and η (Pa*s) were calculated.

Mikula et al, found a mean elastic moduli value of 3.05 Kpa through the axial cornea measured using acoustic radiation force elasticity microscopy [29], in agreement we found an average elastic modulus of 3.44 ± 2.67 Kpa.

Francis et al, reported methodology to obtain corneal viscous properties analyzing the temporal corneal deflection signal from air-puff applanation in a large sample of normal subjects and patients with keratoconus [30]. In particular, they analyzed the deformation data using the Standard Linear Solid and Kelvin-Voigt models, unfortunately they did not detect significant corneal viscous response of the cornea and concluded that viscous properties cannot be computed from air-puff applanation. Our proposed methodology allowed us to experimentally measure (and calculate analytically) the viscous property of the human cornea in vivo, we found an average value for normal corneas of 3.57 ± 2.39 [Pa · s].

Considering that intraocular pressure (IOP) is the main clinically interesting force affecting the cornea (and its implications on the optical nerve and glaucoma disease), Figure 1 explored the influence of IOP on corneal hysteresis (CH). A negative correlation was found between IOP and CH in accordance with previous studies [31–33].

Therefore, the higher the IOP, the lower the CH and therefore the lower the ability of the cornea to dissipate and/or absorb energy from excess of intraocular pressure.

In that sense, the influence of IOP on the separated elastic and viscous components was analyzed in Figure 4.

A piecewise asymmetric linear behavior was found between IOP, E and η . For a IOP threshold value of $IOP_u=14.45$ mmHg. A negative linear correlation between E and η with IOP was found for values of IOP lower than IOP_u . However, for intraocular pressure measurements greater than 14.45 mmHg, both the elastic and viscous components of the cornea increase with IOP.

This seemingly anomalous behavior can be better understood analyzing the results shown in Section 3.2. The corneal retardation has a limit of 1.22 ms from which the corneal elasticity reverses its behavior (Figure 5).

Considering the threshold value of $\tau=1.22$ ms, we investigated the influence of separated elasticity and viscosity on corneal hysteresis. For low values of retardation time, an increase in both elasticity and viscosity implies a growth in CH. But consequently, for retardation times higher than 1.22 ms the dependence of the elastic component on CH decreases and governs a clear correlation of viscosity with corneal hysteresis: as the viscosity increases the CH decreases with negative significant correlation.

Therefore, for corneal retardation times higher than 1.22 ms the cornea shows predominant viscous behavior. That is, the cornea is able to absorb energy but losses the capability of energy dissipation.

Optimal visual acuity is contingent upon corneal transparency. Corneal infections, contact lens complications, chemical injuries or neovascularization are causes of corneal opacification. However, corneal surgery for refractive error correction such as photorefractive keratectomy and accelerated cross-linking for the treatment of degenerative keratoconus can lead to permanent corneal opacification in healthy patients [34]. Those last two corneal surgery techniques involve a redistribution of corneal stiffness and biomechanical remodeling.

In this sense, Section 3.3 analyzed the influence of elastic and viscous components on corneal transparency quantified by optical densitometry measurements (corneal Scheimpflug imaging). The results showed a linear dependence on the optical density (OD), but no statistical relationship with elasticity (See Figure 7). Our findings revealed a decrease in optical transparency (i.e. higher optical density) as the viscosity increases.

The results shown in Figure 8 are especially relevant for refractive surgery to better understand how photorefractive laser ablation redistributes the corneal stiffness and how this affects the appearance of higher order aberrations such as coma.

On the other hand, one-dimension tensile creep and stress relaxation tests are usually performed to analyze the viscoelastic nature of the cornea [35,36]. SLSM allowed us to simulate feedback creep-relaxation tests from calculated experimental data. The creep and relaxation responses of normal (mean value of 200 healthy subjects), ocular hypertensive and Ortho-K contact lens user were compared. The patient with ocular hypertension showed a drastically reduced response in both creep and relaxation responses compared to normal eyes, however the Ortho-K user showed a weak and reduced response in the creep response only.

The results obtained in the creep-relaxation tests can help to better understand the management of glaucoma and the biomechanical impact of the use of Ortho-K contact lenses for the temporal correction of ametropia.

To conclude, we present a new methodology to experimentally derive an analytical expression to calculate corneal viscosity from purely elastic and retardation time biomechanical properties, applying the Standard Linear Solid Model to air-puff measurements.

The average elastic and viscous values were established for a sample of 200 healthy and young subjects. While viscoelastic property is a well-established biomarker of corneal biomechanics, alterations in viscous properties can be masked or confounded by predominantly elastic behaviors. However, the results showed that viscosity plays a fundamental role not only on corneal viscoelasticity but also in optical transparency.

Future work includes a clinical study of the elastic and viscous properties in an ocular hypertension population and patients undergoing refractive surgery.

Author Contributions: Conceptualization, F.A. ; methodology, F.A. and O. B.; software, F.A.; validation, F.A. and O.B.; formal analysis, F.A. and O.B. ; investigation, F.A., O.B. M.C.M. and L.R.; resources, F.A.; data curation, F.A. and O.B.; writing—original draft preparation, F.A. and O.B.; writing—review and editing, F.A. and O.B.; visualization, L.R and M.C.M.; supervision, F.A.; project administration, F.A.; funding acquisition, F.A. All authors have read and agreed to the published version of the manuscript.”

Funding: This research was funded by “Departamento de Ciencia, Universidad y Sociedad del Conocimiento del Gobierno de Aragón (research group E44–23R)”.

Institutional Review Board Statement: The study was conducted in accordance with the Declaration of Helsinki, and approved by the Ethics Committee of the Health Sciences Institute of Aragon, Spain. (protocol code: C.P.-C.I. PI20/377, date of approval: 14 July 2020).

Informed Consent Statement: Informed consent was obtained from all subjects involved in the study.

Data Availability Statement: Dataset is available upon reasonable request.

Conflicts of Interest: The authors declare no conflicts of interest.

References

1. Meek K.M. Corneal collagen – its role in maintaining corneal shape and transparency. *Biophys Rev* 2009, 1:83–93.
2. Espana, E.M.; Birk, D.E. Composition, structure and function of the corneal stroma. *Exp Eye Res* 2020, 198:108137.
3. Meek, K.M.; Knupp, C. Corneal structure and transparency. *Prog Retin Eye Res* 2015, 49:1-16.
4. Bell, J.S.; Hayes, S.; Whitford, C.; Sanchez-Weatherby, J.; Shebanova, O.; Terrill, N.J.; Sørensen, T.L.M.; Elsheikh, A.; Meek, K.M. Tropocollagen springs allow collagen fibrils to stretch elastically. *Acta Biomater* 2022, 1,142:185-193.
5. Chong, J.; Dupps, W.J. Jr. Corneal biomechanics: Measurement and structural correlations. *Exp Eye Res* 2021; 205:108508.
6. Wilson, A.; Marshall, J. A review of corneal biomechanics: Mechanisms for measurement and the implications for refractive surgery. *Indian J Ophthalmol* 2020, 68,12:2679-2690.
7. Marinescu, M.; Dascalescu, D.; Constantin, M.; Coviltir, V.; Burcel, M.; Darabus, D.; Ciuluvica, R.; Stanila, D.; Potop, V.; Alexandrescu, C. Corneal Biomechanics - an Emerging Ocular Property with a Significant Impact. *Maedica (Bucur)* 2022, 17,4,:925-930.
8. Kaushik, S.; Pandav, S.S. Ocular Response Analyzer. *J Curr Glaucoma Pract* 2012, 6,1,:17-19.
9. Lan, G.; Twa, M.D.; Song, C.; Feng, J.; Huang, Y.; Xu, J.; Qin, J.; An, L.; Wei, X. In vivo corneal elastography: A topical review of challenges and opportunities. *Comput Struct Biotechnol J* 2023, 13,21:2664-2687.
10. Eltony, A.M.; Shao, P.; Yun, S.H. Measuring mechanical anisotropy of the cornea with Brillouin microscopy. *Nat Commun* 2022, 15, 13(1):1354.
11. Terai, N.; Raiskup, F.; Haustein, M.; Pillunat, L.E.; Spoerl, E. Identification of biomechanical properties of the cornea: the ocular response analyzer. *Curr Eye Res* 2012, 37(7):553-62.
12. Salouti, R.; Bagheri, M.; Shamsi, A.; Zamani, M. Corneal Parameters in Healthy Subjects Assessed by Corvis ST. *J Ophthalmic Vis Res* 2020, 2, 15(1):24-31.
13. Yun, S.H.; Chernyak, D. Brillouin microscopy: assessing ocular tissue biomechanics. *Current Opinion in Ophthalmology* 2018, 29,4: 299-305.
14. Zhang, H.; Asroui, L.; Tarib, I.; Dupps, W.J. Jr.; Scarcelli, G.; Randleman, J.B. Motion-Tracking Brillouin Microscopy Evaluation of Normal, Keratoconic, and Post-Laser Vision Correction Corneas. *Am J Ophthalmol* 2023, 254:128-140.
15. Ávila, F.J.; Marcellán, M.C.; Remón, L. In Vivo Biomechanical Response of the Human Cornea to Acoustic Waves. *Optics* 2023, 4, 584-594
16. Kobayashi, A.S.; Staberg, L.G.; Schlegel, W.A. Viscoelastic properties of human cornea. *Exp Mech* 1973, 13(12):497–503.
17. Lakes, R.S. Viscoelastic Solids. 1999;15–61.CRC Press Boca Raton, FL.
18. Zimprich, L.; Diedrich, J.; Bleeker, A.; Schweitzer, J.A. Corneal Hysteresis as a Biomarker of Glaucoma: Current Insights. *Clin Ophthalmol* 2020, 10, 14:2255-2264.
19. Glass, D.H.; Roberts, C.J.; Litsky, A.S.; Weber, P.A. A Viscoelastic Biomechanical Model of the Cornea Describing the Effect of Viscosity and Elasticity on Hysteresis. *Invest Ophthalmol Vis Sci* 2008, 49(9):3919-3926.

20. Su, P.; Yang, Y.; Xiao, J.; Song Y. Corneal hyper-viscoelastic model: derivations, experiments, and simulations. *Acta BioengBiomech* 2015, 17(2):73-84.
21. Whitford, C.; Movchan, N.V.; Studer, H.; Elsheikh, A. A viscoelastic anisotropic hyperelastic constitutive model of the human cornea. *Biomech Model Mechanobiol* 2018, 17(1):19-29.
22. Ahmed, H.M.; Salem, N.M.; Al-Atabany, W. Human cornea thermo-viscoelastic behavior modelling using standard linear solid model. *BMC Ophthalmol* 2023, 23, 250.
23. Kelly, P. Solid mechanics part I: an introduction to solid mechanics Solid Mechanics Lecture Notes University of Auckland. 2013, (https://pkel015.connect.amazon.auckland.ac.nz/SolidMechanicsBooks/Part_I/index.html).
24. Liu, J.; Roberts, C.J. Influence of corneal biomechanical properties on intraocular pressure measurement: quantitative analysis. *J Cataract Refract Surg* 2005, 31:146–155.
25. Brinson H.F.; Brinson L.C. Polymer Engineering Science and Viscoelasticity (Springer) 2008.
26. Jannesari, M.; Mosaddegh, P.; Kadkhodaei.; Kasprzak, H.; Jabbarvand Behrouz M. Numerical and clinical investigation on the material model of the cornea in Corvis tonometry tests: differentiation between hyperelasticity and viscoelasticity. *Mech Time Depend Mater* 2018, 23, 373–84.
27. Barco O., Ávila FJ, Marcellán C, Remón L, Corneal retardation time as an ocular hypertension disease indicator. *Biomed Phys. Eng Express* 2024, 10, 015014.
28. Deol, M.; Taylor, D.A.; Radcliffe, N.M. Corneal hysteresis and its relevance to glaucoma. *Curr Opin Ophthalmol* 2015, 26(2):96-102.
29. Mikula, E.R.; Jester, J.V.; Juhasz, T. Measurement of an Elasticity Map in the Human Cornea. *Invest Ophthalmol Vis Sci* 2016, 57(7):3282-6.
30. Francis. M.; Matalia, H.; Nuijts, R.M.M.A.; Haex, B.; Shetty. R.; Sinha Roy, A. Corneal Viscous Properties Cannot Be Determined From Air-Puff Applanation. *J Refract Surg* 2019, 1;35(11):730-736.
31. Dana, D.; Mihaela, C.; Raluca, I.; Miruna. C.; Catalina, I.; Miruna, C.; Schmitzer, S.; Catalina C. Corneal hysteresis and primary open angle glaucoma. *Rom J Ophthalmol* 2015, 59(4):252-254.
32. Nossair, A.A.; Kassem, M.K.; Eltanamly, R.M.; Alahmadawy, Y.A. Corneal Hysteresis, Central Corneal Thickness, and Intraocular Pressure in Rheumatoid Arthritis, and Their Relation to Disease Activity. *Middle East Afr J Ophthalmol* 2021, 31;28(3):174-179.
33. Murtagh, P.; O'Brien, C. Corneal Hysteresis, Intraocular Pressure, and Progression of Glaucoma: Time for a “Hyst-Oric” Change in Clinical Practice? *J Clin Med* 2022, 11, 2895.
34. Blanco-Dominguez, I.; Duch, F.; Reyes, J.; Polo, V.; Abad, J.M.; Gomez-Barrera, M.; Olate-Perez, Á. Permanent corneal opacification after refractive surgery with a combined technique: Photorefractive keratectomy (PRK) and accelerated cross-linking (PRK Xtra) in healthy patients. *J Fr Ophtalmol* 2021, 44(3):e141-e143
35. Abyaneh, M.H.; Wildman, R.D.; Ashcroft, I.A.; Ruiz, P.D. A hybrid approach to determining cornea mechanical properties in vivo using a combination of nano-indentation and inverse finite element analysis. *J Mech Behav Biomed Mater* 2013, 27:239-48.
36. Lombardo, G.; Serrao, S.; Rosati, M.; Lombardo, M. Analysis of the viscoelastic properties of the human cornea using Scheimpflug imaging in inflation experiment of eye globes. *PLoS One* 2014, 14;9(11):e112169.

Disclaimer/Publisher’s Note: The statements, opinions and data contained in all publications are solely those of the individual author(s) and contributor(s) and not of MDPI and/or the editor(s). MDPI and/or the editor(s) disclaim responsibility for any injury to people or property resulting from any ideas, methods, instructions or products referred to in the content.